

# Differentially Coherent Combining for Double-Dwell Code Acquisition in DS-CDMA Systems

Oh-Soon Shin, *Student Member, IEEE*, and Kwang Bok (Ed) Lee, *Member, IEEE*

**Abstract**—The use of differentially coherent combining is proposed to improve the performance of a double-dwell acquisition system by increasing the reliability of a decision in the verification stage. The detection and mean acquisition time performance of the acquisition scheme with the proposed combining scheme is analyzed in frequency-selective Rayleigh fading channels, and compared with that of two previously published double-dwell acquisition schemes based on long correlation intervals and noncoherent combining. It is shown that the proposed acquisition scheme outperforms the previous ones, and that the performance improvement increases as the frequency offset increases.

**Index Terms**—Acquisition, differentially coherent combining, double-dwell search, direct-sequence code-division multiple access (DS-CDMA), frequency offset.

## I. INTRODUCTION

IN DIRECT-SEQUENCE code-division multiple-access (DS-CDMA) systems, code synchronization is one of the most important parts. Code synchronization is usually achieved in two steps: acquisition for coarse alignment and tracking for fine alignment; the former is addressed in this letter. In the design of acquisition systems, an important goal is to reduce mean acquisition time, which is the average time that elapses prior to acquisition.

Various acquisition schemes have been investigated for rapid acquisition [1]. One approach to achieving fast acquisition is to use a double-dwell scheme rather than a single-dwell scheme [1], [2]. The advantage of the double-dwell scheme results from the significant reduction of costly false alarms. A double-dwell scheme has two stages of operation: search and verification. The former is used to make a tentative decision on the received code phase, and the latter is used to verify the decision in the search stage. Therefore, it is desirable that the decisions in the verification stage should be reliable to avoid false alarms. A simple method to increase reliability is to increase the correlation intervals of the correlator in the verification stage. However, the performance of this scheme is degraded severely in the presence of frequency offset and fading [2].

To overcome the problem in increasing the correlation intervals, verification methods based on multiple observations have

been investigated [2]–[4]. In these methods, a number of correlations are performed to obtain multiple observations for the cell under the test. The performance of this approach depends on how to decide whether the cell is the in-phase cell or not, using these observations. A majority logic-type decision strategy has been investigated in [3], where each observation is independently tested, and the decision is made based on the number of observations passing the test. Although this scheme is more robust than the method of increasing the correlation intervals, the performance of this scheme may be poor in the presence of severe frequency offset and/or fading. This is because in these environments, the result of each test becomes too unreliable for the majority logic decision to be effective. Another type of decision strategy is presented in [2] and [4], where the decision is made based on only one test using the decision variable formed by noncoherent combining of multiple observations. The noncoherent combining inherently increases the reliability of the decision variable. In [5], the performance of these two verification methods has been compared, and it has been found that the decision based on the noncoherent combining outperforms the majority logic-type decision.

Recently, a differentially coherent combining scheme has been proposed in [6] and [7] as an effective method to combine multiple observations for slot synchronization in wideband CDMA (W-CDMA) systems. In [6] and [7], it has been shown that this combining scheme is superior to the noncoherent combining scheme in the presence of frequency offset and fading. Motivated by this investigation, we propose employing the differentially coherent combining instead of the noncoherent combining in the verification stage for a double-dwell acquisition system. In the proposed acquisition system, differential processing is performed on multiple observations, and the outputs of the differential processing are combined to form a decision variable in the verification stage. The detection and mean acquisition time performance of the proposed acquisition scheme is analyzed in frequency-selective Rayleigh fading channels, and it will be shown that the proposed acquisition scheme outperforms the previously considered double-dwell acquisition schemes.

## II. PROPOSED ACQUISITION SYSTEM

The proposed acquisition system is a double-dwell system with search and verification stages, as depicted in Fig. 1, and it can be employed for either the downlink or uplink of a DS-CDMA system. The code period  $NT_c$  is discretized with a step size of  $T_c$ , the chip duration, resulting in  $N$  cells of the uncertainty region. In the search stage, the decision variable  $S$  corresponding to each test cell is collected using

Paper approved by L. Wei, the Editor for Wireless CDMA Systems of the IEEE Communications Society. Manuscript received January 9, 2002; revised June 15, 2002 and December 3, 2002. This work was supported by the Brain Korea 21 Project. This paper was presented in part at the 12th IEEE Symposium on Personal, Indoor, and Mobile Radio Communications, San Diego, CA, September–October, 2001.

The authors are with the School of Electrical Engineering and Computer Science, Seoul National University, Seoul 151–742, Korea (e-mail: osshin@mobile.snu.ac.kr; klee@snu.ac.kr).

Digital Object Identifier 10.1109/TCOMM.2003.814205

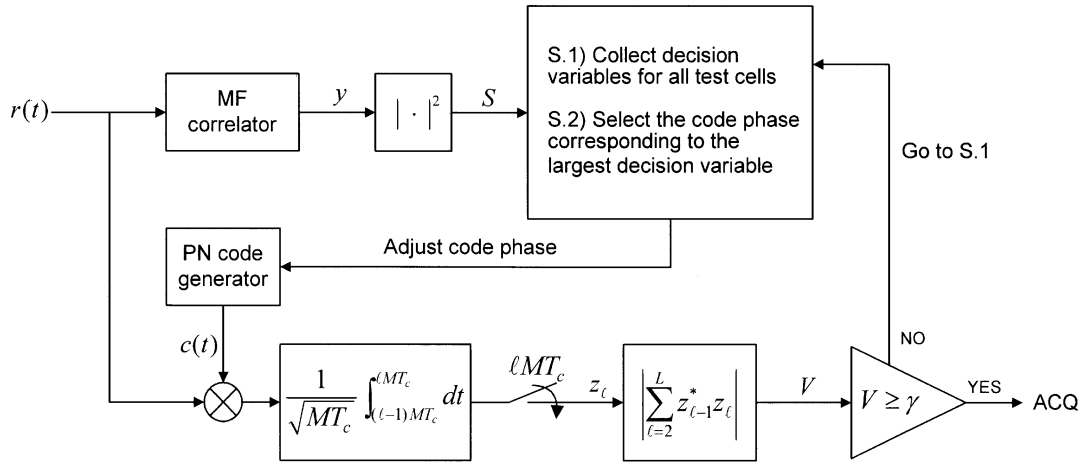


Fig. 1. Proposed acquisition system.

a matched-filter correlator with a correlation interval of  $M$  chips, and the code phase corresponding to the largest decision variable is tentatively assumed as the in-phase cell. In the verification stage, an active correlator with a correlation interval of  $M$  chips performs a number of correlations for the cell selected in the search stage. To form a decision variable in the verification stage,  $L$  successive observations, i.e., correlator outputs, denoted as  $z_\ell$ ,  $\ell = 1, 2, \dots, L$  in Fig. 1, are combined after differential processing,  $Z_{\ell-1}^* Z_\ell$ . Hence, the decision variable  $V$  in the verification stage is expressed as

$$V = \left| \sum_{\ell=2}^L z_{\ell-1}^* z_\ell \right|. \quad (1)$$

This decision variable is compared with a decision threshold  $\gamma$ . If the decision variable exceeds the threshold, acquisition is declared and the tracking system is enabled. Otherwise, the acquisition system goes back to the search stage. In contrast to the proposed acquisition system, the decision variable for the double-dwell acquisition system based on the noncoherent combining is formed as  $V = \sum_{\ell=1}^L |z_\ell|^2$  [2], [4].

The benefit of differentially coherent combining is due to the differential processing prior to combining. The summation in (1) may be viewed as a coherent combining, since the signal components corrupted by fading and frequency offset are nearly phase aligned by differential processing, if fading is slow enough not to vary significantly over two consecutive correlation intervals. Since this assumption is valid in typical environments [6], the differentially coherent combining may be almost as robust to fading as the noncoherent combining. Hence, the differentially coherent combining may provide greater combining gain than the noncoherent combining, even in the presence of fading and frequency offset. The absolute value operation in (1) after the summation is employed in order to capture signal components split into real and imaginary parts by the frequency offset [6]. The differential processing is also more effective in reducing the effects of background noise and interference than the squaring operation in the noncoherent combining [8]. Consequently, the proposed acquisition scheme is expected to provide shorter mean acquisition time than the scheme based on the noncoherent combining.

### III. PERFORMANCE ANALYSIS

In this section, the performance of the acquisition system described in Section II is analyzed in frequency-selective Rayleigh fading channels. Acquisition is assumed if any of the resolvable paths are acquired. The received signal model is described in Section III-A, and equations for the probabilities of detection and false alarm are derived in Section III-B. An expression for the mean acquisition time is presented in Section III-C.

#### A. Received Signal Model

It is assumed that a DS-CDMA signal is received from a pilot channel without data modulation, and the receiver is chip synchronized to the received signal. The complex baseband equivalent of the received signal may be expressed as

$$r(t) = \sqrt{P} \cdot \sum_{\kappa=1}^{L_p} \alpha_\kappa(t) e^{j2\pi f_o t} c(t - \tau_\kappa) + n(t) \quad (2)$$

where  $P$  is the average received signal power,  $f_o$  is the frequency offset between transmitter and receiver,  $c(t)$  is the pseudonoise (PN) code waveform with period of  $N$  chips,  $\tau_\kappa$  is the received code phase for the  $\kappa$ th resolvable path, and  $L_p$  is the number of resolvable paths. The multiplicative Rayleigh fading channel for the  $\kappa$ th resolvable path is denoted as  $\alpha_\kappa(t)$ , which is a complex Gaussian random process with the autocorrelation function given as  $E[\alpha_\kappa(t) \alpha_\kappa^*(\tau)] = \Omega(\kappa) \cdot J_o(2\pi f_D |t - \tau|)$  [9], where  $\Omega(\kappa)$  is the multipath intensity profile normalized as  $\sum_{\kappa=1}^{L_p} \Omega(\kappa) = 1$ ,  $J_\kappa(\cdot)$  represents the  $\kappa$ th-order Bessel function of the first kind, and  $f_D$  is the Doppler spread. The noise plus interference from other users, denoted as  $n(t)$ , is a complex additive white Gaussian noise (AWGN) process with one-sided power spectral density  $N_0$ .

#### B. Probabilities of Detection and False Alarm

1) *Search Stage:* As depicted in Fig. 1, the decision variable  $S$  in the search stage is formed by squaring a matched-filter output  $y$ :  $S = |y|^2$ . The probability density function (pdf) and

cumulative distribution function (cdf) of  $S$  under the hypothesis  $H_n$ ,  $n = 11, 12, \dots, 1L_p$ , 0 can be written as [10]

$$f_S(r|H_n) = \frac{1}{\lambda_n} \exp\left(-\frac{r}{\lambda_n}\right), F_S(r|H_n) = 1 - \exp\left(-\frac{r}{\lambda_n}\right) \quad (3)$$

where  $H_{1\kappa}$ ,  $\kappa = 1, 2, \dots, L_p$  and  $H_0$  denote the hypotheses corresponding to the in-phase cell associated with the  $\kappa$ th resolvable path and an out-of-phase cell, respectively. Under the assumption that the multipath interference is negligible, the conditional first moment of  $S$  for the given hypothesis  $H_n$ , denoted as  $\lambda_n$ , can be calculated for each hypothesis as

$$\begin{aligned} \lambda_{1\kappa} &\triangleq E[S = |y|^2 | H_{1\kappa}] \\ &= \frac{1}{MT_c} E \left[ \int_0^{MT_c} \int_0^{MT_c} r(t)c(t-\tau_\kappa)r^*(s)c(s-\tau_\kappa) dt ds \right] \\ &= \frac{P}{MT_c} \int_0^{MT_c} \int_0^{MT_c} E[\alpha_\kappa(t)\alpha_\kappa^*(s)] e^{j2\pi f_o(t-s)} dt ds \\ &\quad + \frac{1}{MT_c} \int_0^{MT_c} \int_0^{MT_c} E[n(t)n^*(s)] c(t-\tau_\kappa)c(s-\tau_\kappa) dt ds \\ &= \frac{P\Omega(\kappa)}{MT_c} \int_{-MT_c}^{MT_c} J_0(2\pi f_D \xi) e^{j2\pi f_o \xi} (MT_c - |\xi|) d\xi + N_0 \\ &\cong \frac{P\Omega(\kappa)}{MT_c} \sum_{m=-M}^{M-1} J_0(2\pi m f_D T_c) e^{j2\pi m f_o T_c} (M - |m|) T_c^2 + N_0 \\ &= P\Omega(\kappa) T_c \\ &\quad \cdot \left( 1 + 2 \sum_{m=1}^{M-1} J_0(2\pi m f_D T_c) \cos(2\pi m f_o T_c) \left(1 - \frac{m}{M}\right) \right) + N_0 \end{aligned} \quad (4)$$

and

$$\lambda_0 \triangleq E[S = |y|^2 | H_0] = PT_c + N_0 \quad (5)$$

where the first term  $PT_c$  in the right-hand side of (5) represents the self interference due to out-of-phase correlation of the PN sequence [11], and  $PT_c/N_0$  is defined as the signal-to-interference ratio per chip (SIR/chip). The probability of detection  $P_{D1}(\kappa)$  at the  $\kappa$ th resolvable path in the search stage is the probability that the decision variable associated with the  $\kappa$ th resolvable path is the largest among  $N$  decision variables, and thus it may be calculated using (3) as

$$P_{D1}(\kappa) = \int_0^\infty f_S(r|H_{1\kappa}) \left( \prod_{m=1, m \neq \kappa}^{L_p} F_S(r|H_{1m}) \right) (F_S(r|H_0))^{N-L_p} dr. \quad (6)$$

A false alarm corresponds to a situation where the decision variable for an out-of-phase cell is the largest, or any of the decision variables for in-phase cells is not the largest. Thus, the probability of false alarm  $P_{F1}$  in the search stage is calculated as

$$P_{F1} = 1 - \sum_{\kappa=1}^{L_p} P_{D1}(\kappa). \quad (7)$$

2) *Verification Stage:* The decision variable  $V$  in the verification stage is constructed by combining  $L$  observations,  $z_\ell$ ,

$\ell = 1, 2, \dots, L$ , as described in (1). The pdf and cdf of  $V$  under the hypothesis  $H_n$  are expressed as [6]

$$\begin{aligned} f_V(r|H_n) &= \frac{r}{2\pi} \int_0^\infty \int_{-\pi}^\pi \rho \Phi_{V_I V_Q}(\rho \cos \phi, \rho \sin \phi | H_n) J_0(\rho r) d\phi d\rho \\ F_V(r|H_n) &= \frac{r}{2\pi} \int_0^\infty \int_{-\pi}^\pi \Phi_{V_I V_Q}(\rho \cos \phi, \rho \sin \phi | H_n) J_1(\rho r) d\phi d\rho \end{aligned} \quad (8)$$

where  $V_I$  and  $V_Q$  are, respectively, the real and imaginary parts of  $\sum_{\ell=2}^L z_{\ell-1}^* z_\ell$ .  $\Phi_{V_I V_Q}(\cdot, \cdot | H_n)$  represents the joint characteristic function of  $V_I$  and  $V_Q$  under the hypothesis  $H_n$ , which is expressed as

$$\Phi_{V_I V_Q}(\mu, \nu | H_n) = [\det(\mathbf{I} - j\mathbf{R}_n(\mu\mathbf{Q}_I + \nu\mathbf{Q}_Q))]^{-1} \quad (9)$$

where  $\mathbf{Q}_I$  and  $\mathbf{Q}_Q$  are, respectively, the matrices for constructing  $V_I$  and  $V_Q$  from the observation vector  $\mathbf{z} = [z_1, z_2, \dots, z_L]^T$ , i.e.,  $V_I = \mathbf{z}^H \mathbf{Q}_I \mathbf{z}$ ,  $V_Q = \mathbf{z}^H \mathbf{Q}_Q \mathbf{z}$  [6].  $\mathbf{I}$  denotes the  $L$ -dimensional identity matrix,  $\mathbf{R}_n \triangleq E[\mathbf{z}\mathbf{z}^H | H_n]$  is the covariance matrix of  $\mathbf{z}$  under the hypothesis  $H_n$ , and the  $(k, \ell)$  elements of  $\mathbf{R}_{1\kappa}$  and  $\mathbf{R}_0$  can be calculated in a similar manner as in (4)

$$\begin{aligned} (\mathbf{R}_{1\kappa})_{k\ell} &= E[z_k z_\ell^* | H_{1\kappa}] = PT_c \Omega(\kappa) e^{j2\pi(k-\ell)Mf_o T_c} \\ &\quad \cdot \sum_{m=-M}^{M-1} J_0(2\pi((k-\ell)M+m)f_D T_c) \\ &\quad \cdot e^{j2\pi m f_o T_c} \left(1 - \frac{|m|}{M}\right) + N_0 \cdot \delta[k-\ell] \end{aligned} \quad (10)$$

$$(\mathbf{R}_0)_{k\ell} = E[z_k z_\ell^* | H_0] = (PT_c + N_0) \cdot \delta[k-\ell] \quad (11)$$

where  $\delta[k]$  denotes the Kronecker delta function, defined as one for  $k = 0$ , and zero otherwise. From (8), the probability of detection  $P_{D2}(\kappa)$  at the  $\kappa$ th resolvable path and that of false alarm  $P_{F2}$  in the verification stage can be calculated as

$$P_{D2}(\kappa) = 1 - F_V(\gamma | H_{1\kappa}), \quad P_{F2} = 1 - F_V(\gamma | H_0) \quad (12)$$

where  $\gamma$  is the decision threshold.

### C. Mean Acquisition Time

The mean acquisition time is the overall mean time it takes for the search and verification stages to declare acquisition, and it can be calculated using the flow-graph method in [3]. From the reduced state diagram depicted in Fig. 2, the transfer function  $H(z)$  from the "TEST" state to the "ACQ" state is found as

$$H(z) = \frac{H_D(z)}{1 - H_M(z)} \quad (13)$$

where

$$H_D(z) = P_D z^{(N+M-1+LM)T_c} \quad (14)$$

$$\begin{aligned} H_M(z) &= (1 - P_D - P_F) z^{(N+M-1+LM)T_c} \\ &\quad + P_F z^{(N+M-1+LM+K)T_c} \end{aligned} \quad (15)$$

$$P_D = \sum_{\kappa=1}^{L_p} P_{D1}(\kappa) P_{D2}(\kappa), P_F = P_{F1} P_{F2}. \quad (16)$$

In (14) and (15), note that  $(N+M-1)T_c$  is the time required to collect  $N$  decision variables in the search stage with  $(M-1)T_c$

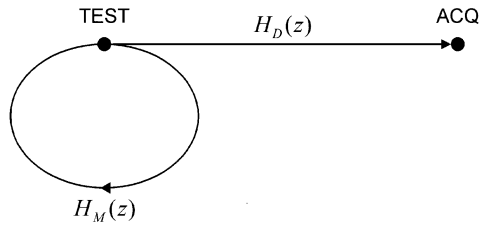


Fig. 2. Reduced state diagram.

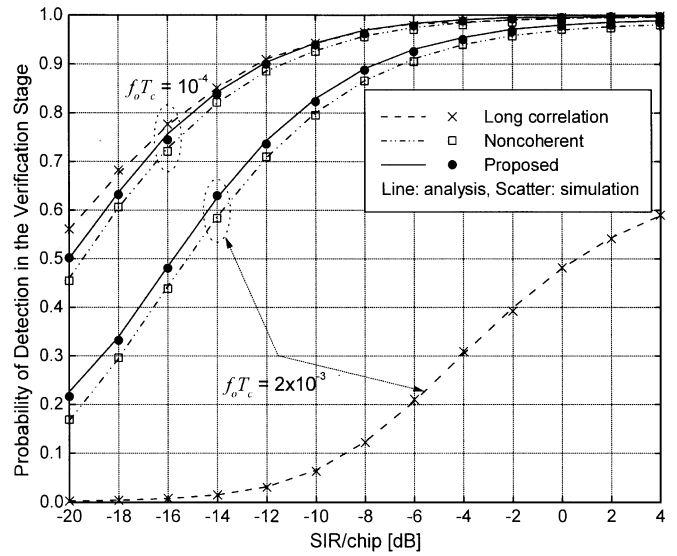
comprising the initialization time of the matched filter.  $LMT_c$  is the time required to obtain  $L$  observations in the verification stage, and  $KT_c$  is the penalty time due to a false alarm. The overall probability of detection  $P_D$  and that of false alarm  $P_F$  are defined in (16). Using (13)–(16), the mean acquisition time can be calculated as

$$\begin{aligned} E[T_{ACQ}] &= \left. \frac{dH(z)}{dz} \right|_{z=1} \\ &= \frac{H'_D(1) + H'_M(1)}{H_D(1)} \\ &= \frac{N + M - 1 + LM + KP_F}{P_D} T_c. \end{aligned} \quad (17)$$

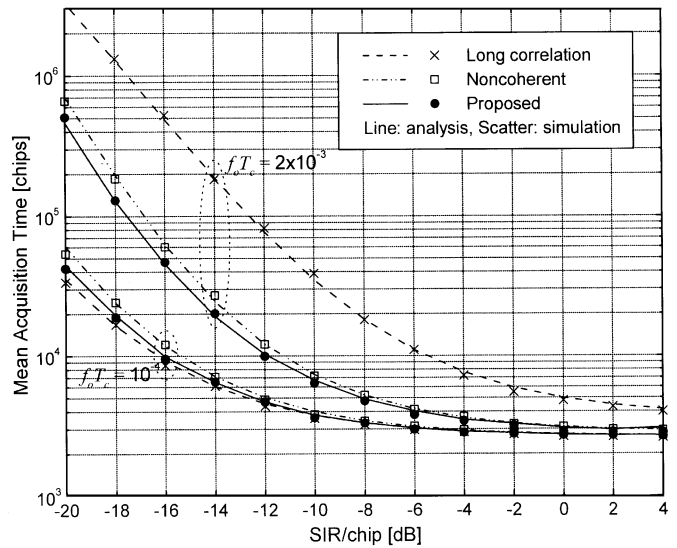
#### IV. NUMERICAL AND SIMULATION RESULTS

In this section, the detection and mean acquisition time performance of the proposed acquisition scheme analyzed in Section III is evaluated and compared with that of two previous double-dwell acquisition schemes described in Section I: the scheme of increasing the correlation intervals to  $LM$  chips in the verification stage, and the scheme based on the noncoherent combining. In this section, these two previous schemes will be referred to as the “long correlation” scheme and “noncoherent” scheme, respectively. The performance of the two previous double-dwell schemes can easily be evaluated using (6), (7), (12), (16), and (17) with corresponding pdf and cdf equations [6]. The code period  $N$  and the correlation length  $M$  are set to 1024 and 256, respectively, and the penalty time  $K$  is assumed to be  $10^5$  chips.

Fig. 3 compares the detection and mean acquisition time performance of the three schemes in a frequency-nonselctive fading channel with  $L_p = 1$ , when the number of observations  $L = 5$  and the normalized Doppler spread  $f_D T_c = 10^{-4}$ . A close agreement between simulation and numerical results verifies the correctness of the performance analysis. The probability of detection  $P_{D2}$  in the verification stage is depicted in Fig. 3(a), which is obtained from (12) with corresponding cdf equations for each scheme. Only the verification stage is considered in this figure, since the search stage is identical for all three schemes. For fair comparisons, the decision threshold  $\gamma$  is set so that the probability of false alarm  $P_{F2}$  becomes a constant value  $10^{-3}$  for each scheme. In Fig. 3(a), it is observed that the proposed scheme provides greater probability of detection than the noncoherent scheme. This indicates that the differentially coherent combining used in the proposed acquisition scheme provides greater combining gain than the noncoherent combining. The long correlation scheme performs well for the normalized frequency offset  $f_o T_c = 10^{-4}$ , but performs much worse than the other schemes for  $f_o T_c = 2 \times 10^{-3}$ .



(a)



(b)

Fig. 3. Performance comparisons for  $L_p = 1$ ,  $L = 5$ , and  $f_D T_c = 10^{-4}$ . (a) Probability of detection in the verification stage. (b) Mean acquisition time.

This is because of a significant phase rotation of the signal component during the correlation interval of  $LM$  chips for large frequency offset.

Fig. 3(b) shows the mean acquisition time performance. In this figure, the decision threshold  $\gamma$  is numerically determined to minimize the mean acquisition time for each condition. It is shown that the proposed acquisition scheme outperforms the noncoherent scheme. This performance improvement is due to better detection performance provided by the differentially coherent combining as shown in Fig. 3(a). Fig. 4 compares the mean acquisition time performance in a frequency-selective fading channel with  $L_p = 6$ , when  $L = 5$  and  $f_D T_c = 10^{-4}$ . We use ITU-R Vehicular A channel model [12] with multipath intensity profile given as  $\Omega(1) = 0.4850$ ,  $\Omega(2) = 0.3853$ ,  $\Omega(3) = 0.0611$ ,  $\Omega(4) = 0.0485$ ,  $\Omega(5) = 0.0153$ , and  $\Omega(6) = 0.0049$ . The decision threshold  $\gamma$  is determined in the same manner as in Fig. 3(b). Simulation results as well

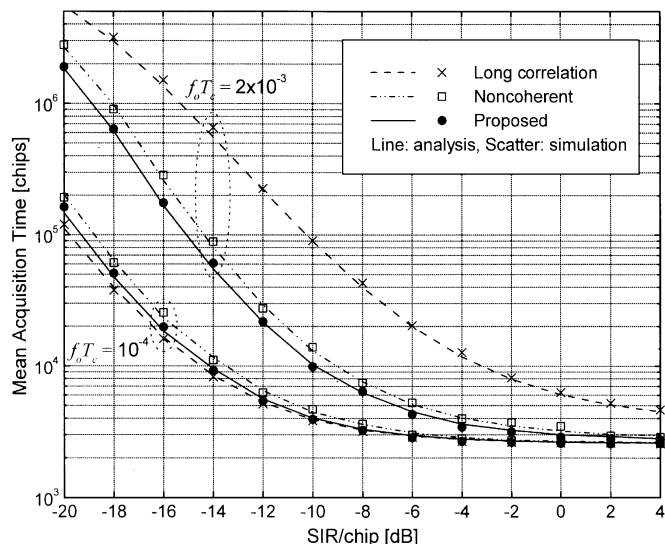


Fig. 4. Mean acquisition time performance comparisons for  $L_p = 6$ ,  $L = 5$ , and  $f_D T_c = 10^{-4}$ .

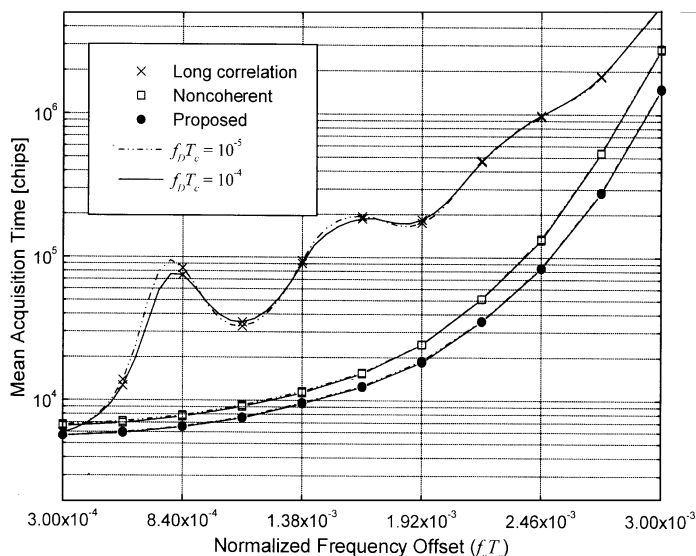


Fig. 5. Effects of the Doppler spread and frequency offset on mean acquisition time for  $L_p = 6$ ,  $L = 5$ , and  $\text{SIR}/\text{chip} = -12$  dB.

as numerical results are provided to validate the performance analysis. Similar performance trends can be observed as for the frequency-nonsselective fading channel in Fig. 3(b).

The effects of the Doppler spread and frequency offset on mean acquisition time are depicted in Fig. 5, when  $L_p = 6$ ,  $L = 5$ , and  $\text{SIR}/\text{chip} = -12$  dB. The results are obtained from numerical analysis. The channel model used in this figure is the same as that used in Fig. 4, and the decision threshold  $\gamma$  is determined in the same manner as in Fig. 4. The effects of Doppler spread on the performance are observed to be negligible for all three schemes in this figure. This is because the variation of the fading process is not significant during the second dwell time  $LMT_c$ , even when the normalized Doppler spread  $f_D T_c$  is as large as  $10^{-4}$  corresponding to  $f_D = 368.64$  Hz for the chip rate of 3.6864 MHz [13]. This also implies that the differentially coherent combining is as robust to fading as the noncoherent combining in typical environments, as discussed in Section II. Fig. 5, on the other hand, shows that the mean acquisition time performance is severely degraded by the

frequency offset. Note that the frequency offset range ( $3 \times 10^{-4}$ ,  $3 \times 10^{-3}$ ) considered in this figure is reasonable in practical situations, since  $f_o T_c = 3 \times 10^{-3}$  corresponds to  $f_o = 11$  kHz (5.5 ppm at 2 GHz carrier frequency) for the chip rate of 3.6864 MHz. The long correlation scheme is found to be much more susceptible to the frequency offset than the other schemes. The oscillatory phenomenon of the mean acquisition time is caused by the oscillation of signal components in the correlator outputs with the frequency offset [6]. It is shown that the proposed acquisition scheme outperforms the previous ones, and that the performance difference becomes greater as the frequency offset increases. Similar performance trends are observed for other values of SIR/chip, although we do not present the results. When  $\text{SIR}/\text{chip} = -12$  dB,  $f_o T_c = 3 \times 10^{-3}$ , and  $f_D T_c = 10^{-4}$ , the mean acquisition time of the proposed scheme is  $1.5 \times 10^6$  chips, and that of the noncoherent scheme is  $2.8 \times 10^6$  chips. In this case, the use of the proposed acquisition scheme produces about a 50% reduction in the mean acquisition time, compared with the noncoherent.

## V. CONCLUSION

In this letter, the use of a differentially coherent combining scheme has been proposed for the verification stage of the double-dwell acquisition scheme. The detection and mean acquisition time performances have been analyzed in frequency-selective Rayleigh fading channels, and compared with those of previously considered double-dwell schemes. It has been shown that the proposed acquisition scheme outperforms the previous ones, and that the performance improvement becomes greater as the frequency offset increases.

## REFERENCES

- [1] M. K. Simon, J. K. Omura, R. A. Scholtz, and B. K. Levitt, *Spread Spectrum Communications Handbook*. New York: McGraw-Hill, 1994.
- [2] A. J. Viterbi, *CDMA: Principles of Spread Spectrum Communication*. New York: Addison-Wesley, 1995.
- [3] A. Polydoros and C. Weber, "A unified approach to serial search spread-spectrum code acquisition—Parts I and II," *IEEE Trans. Commun.*, vol. COM-32, pp. 542–560, May 1984.
- [4] H.-R. Park, "A parallel code acquisition technique for  $M$ -ary orthogonal signals in a cellular CDMA system," *IEEE Trans. Veh. Technol.*, vol. 49, pp. 2003–2012, Sept. 2000.
- [5] H. G. Kim, I. Song, Y. U. Lee, S. C. Kim, and Y. H. Kim, "Double-dwell serial-search code acquisition using a nonparametric detector in DS-SS systems," in *Proc. IEEE Military Communications Conf. (MILCOM '99)*, Nov. 1999, pp. 571–574.
- [6] Y. K. Jeong, O.-S. Shin, and K. B. Lee, "Fast slot synchronization for intercell asynchronous DS-SS systems," *IEEE Trans. Wireless Commun.*, vol. 1, pp. 353–360, Apr. 2002.
- [7] Y. K. Jeong, K. B. Lee, and O.-S. Shin, "Differentially coherent combining for slot synchronization in intercell asynchronous DS/SS systems," in *Proc. IEEE Int. Symp. Personal, Indoor and Mobile Radio Communications (PIMRC 2000)*, Sept. 2000, pp. 1405–1409.
- [8] M. H. Zarrabizadeh and E. S. Sousa, "A differentially coherent PN code acquisition receiver for CDMA systems," *IEEE Trans. Commun.*, vol. 45, pp. 1456–1465, Nov. 1997.
- [9] W. C. Jakes, *Microwave Mobile Communications*. New York: Wiley, 1974.
- [10] J. G. Proakis, *Digital Communications*, 3rd ed. New York: McGraw-Hill, 1995.
- [11] B. B. Ibrahim and A. H. Aghvami, "Direct sequence spread spectrum matched filter acquisition in frequency-selective Rayleigh fading channels," *IEEE J. Select. Areas Commun.*, vol. 12, pp. 885–890, June 1994.
- [12] "Guidelines for Evaluation of Radio Transmission Technologies (RTT) for IMT-2000," International Telecommun. Union (ITU), Rec. ITU-R M.1225, 1997.
- [13] "Physical Layer Standard for cdma2000 Spread Spectrum Systems," 3rd Generation Partnership Project 2, 3GPP2 C.S0002-A, 2000.